

## Supporting Information Section

# Self-assembly of the non-planar Fe(III) phthalocyanine small-molecule: unraveling the impact on the magnetic properties of organic nanowires

*A. Nicolas Filippin,<sup>1</sup> Victor Lopez-Flores,<sup>1\*</sup> T. Cristina Rojas,<sup>1</sup> Zineb Saghi,<sup>2,3</sup> Victor J. Rico,<sup>1</sup> Juan R. Sanchez-Valencia,<sup>1</sup> Juan P. Espinos,<sup>1</sup> Andrea Zitolo,<sup>4</sup> Michel Viret,<sup>5</sup> Paul A. Midgley,<sup>2</sup> Angel Barranco,<sup>1</sup> Ana Borrás<sup>1\*</sup>*

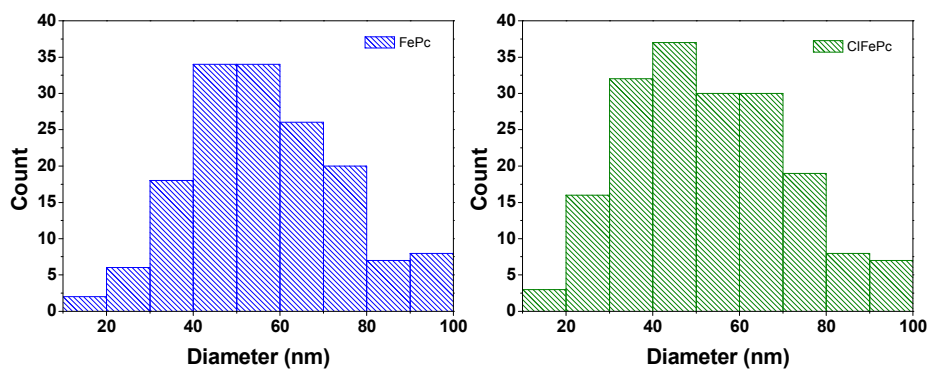
<sup>1</sup> Nanotechnology on Surfaces Laboratory, Instituto de Ciencia de Materiales de Sevilla, CSIC-Universidad de Sevilla, c/Américo Vespucio 49, 41092 Sevilla (Spain)

<sup>2</sup>Department of Materials Science and Metallurgy, University of Cambridge, 27 Charles Babbage Road, CB3 0FS, Cambridge (United Kingdom)

<sup>3</sup> University of Grenoble Alpes, Grenoble F-38000; CEA, LETI, MINATEC Campus, Grenoble F-38054 (France)

<sup>4</sup> Synchrotron SOLEIL, L'Orme des Merisiers, BP 48 Saint Aubin, Gif-sur-Yvette (France)

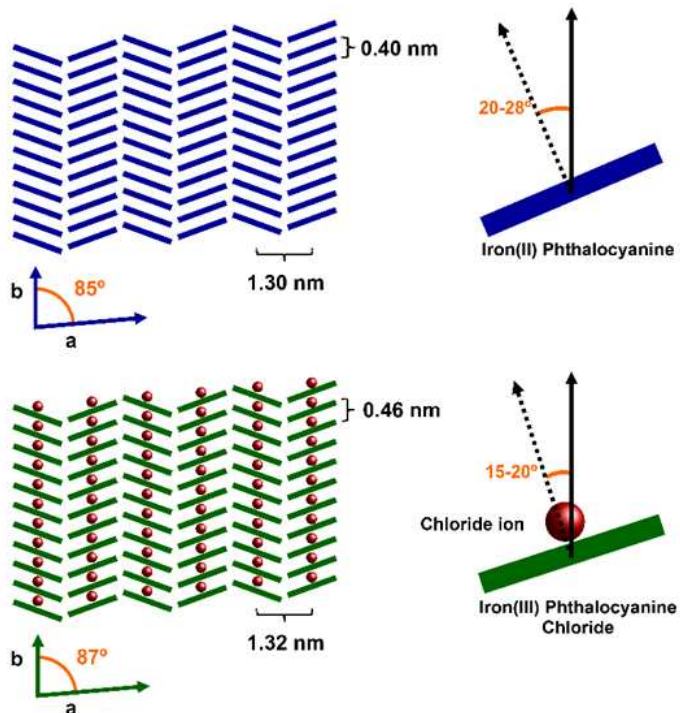
<sup>5</sup> ~~Service de Physique de l'État Condensé (CNRS URA 2464), CEA Saclay,~~ Gif-sur-Yvette (France)



	N total	Mean (nm)	Std Deviation (nm)	Minimum	Median	Maximum
FePc NWs	156	57	18	20	55	118
FePcCl NWs	182	53	18	19	50	98

**Figure S1.** Histograms and statistic data regarding the diameter of the ONWs estimated after digital analysis of several SEM micrographs for each type of phthalocyanine (ImageJ software).

## Section S1. Molecular arrangements in the FePc and FePcCl NWs.



**Schematic S1.** Schematic of the proposed molecular arrangements in the self-assembled FePc and FePcCl nanowire single crystals

## Section S2. Grazing Angle X-ray Diffraction

**Grazing Angle X-ray diffraction** diagrams were recorded in order to find the diffraction peaks coming from the single crystal nanowires. They were taken with a PANalytical X'Pert Pro, in glancing angle mode at 0.2°, from 3 to 50°, at 0.05° step size, using the Cu-K<sub>α</sub> radiation.

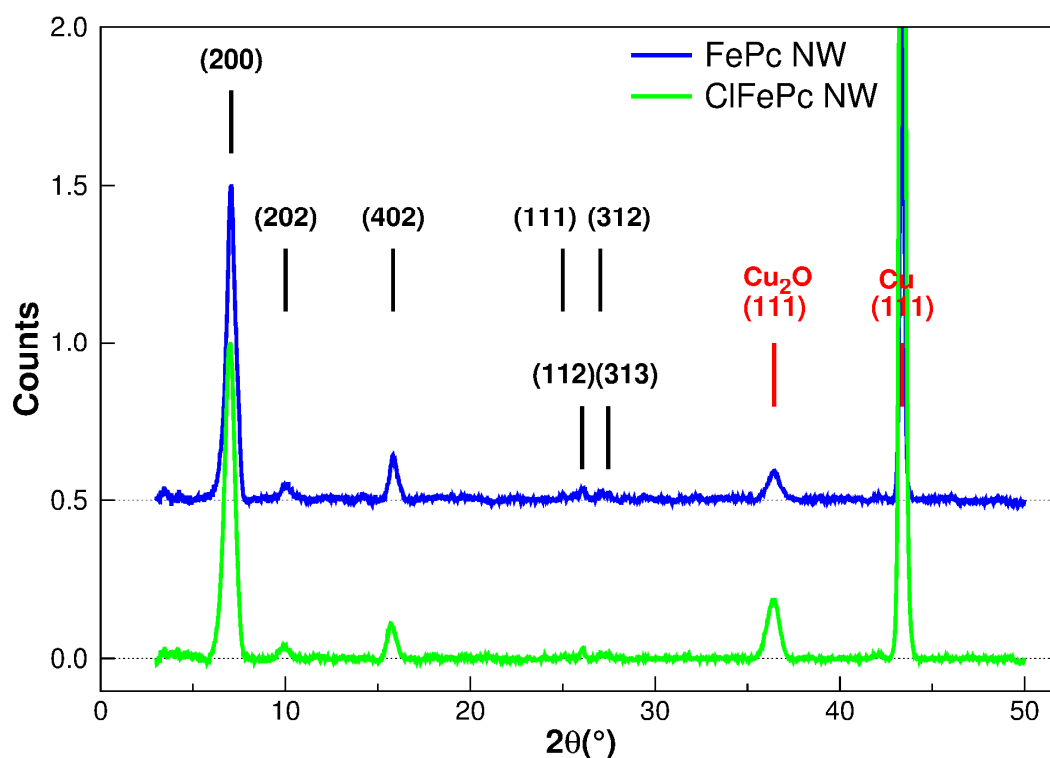


**Figure S2:** Grazing incidence X-ray diffraction diagrams of the FePc nanowire (blue) and FePcCl nanowire (green) samples. The FePc and FePcCl peaks are indexed to their corresponding planes (in black), together with the peaks corresponding to the substrate planes (red)

**Table S1:** Summary of the diffraction peaks and their corresponding planes and interplanar distances for the FePc and FePcCl nanowires samples.

Plane	2 $\theta$ (°) (FePc NW)	$d_{hkl}$ (nm) (FePc NW)	2 $\theta$ (°) (FePcCl NW)	$d_{hkl}$ (nm) (FePcCl NW)
(200)	7.05	1.252	6.98	1.266
(202)	10.01	0.884	9.94	0.890
(402)	15.82	0.561	15.72	0.564
(111)	25.01	0.356	25.01	0.356
(112)	26.05	0.342	26.05	0.342
(321)	27.04	0.329	27.04	0.329
(313)	27.47	0.324	27.47	0.324
Cu <sub>2</sub> O (111)	36.45	0.246	36.45	0.246
Cu (111)	43.38	0.209	43.38	0.209

### Section S3. X-Ray Spectroscopy: X-ray Absorption (XAS); Extended X-Ray Absorption Fine Structure (EXAFS) and X-ray Absorption Near Edge Structure (XANES)

The model for the FePc bulk crystal reference spectrum is constructed similarly to the CuPc EXAFS study from Carrera,<sup>2</sup> by taking the starting coordination distances and angles from the ones obtained in diffraction experiments.<sup>3,4</sup> The single scattering paths were taken up to the Fe-C(2) coordination shell, each of them with coordination numbers fixed to the expected values, and

independent variables accounting for the scattering distances,  $R$ , and Debye-Waller factors,  $\sigma^2$ . Multiple scattering paths were taken when their relative amplitude were above 20%. These include only the ones co-linear or almost co-linear with 3 of 4 legs, that link C(1) and C(2) through N(1) and C(1) atoms. See Figure S2 for a scheme of the scattering paths chosen. Degeneracy of these paths are again fixed due to the fixed coordination numbers, while the effective coordination distances are calculated from the corresponding distances of the single scattering ones, and the Debye-Waller factors are taken as the same as the corresponding farthest coordination shell involved.<sup>2,4</sup> All paths share the same  $S_0^2$  factor and the energy correction  $\Delta E_0$ . This makes 10 the number of variables, which is far below the maximum possible independent variables that can be used given by the Nyquist criterions.<sup>5,6</sup>

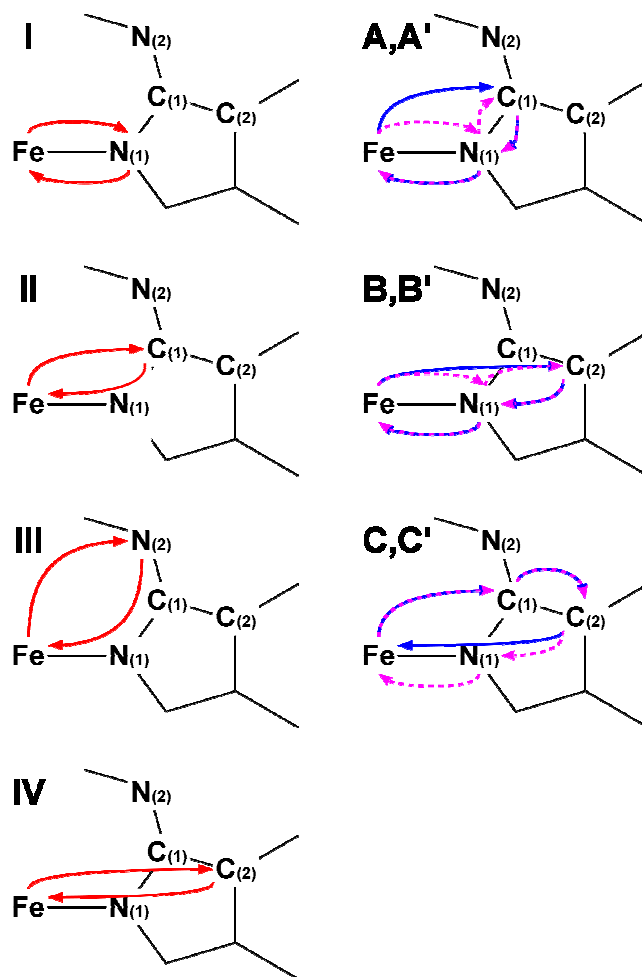


**Figure S3:** Scattering paths on the plane of the phthalocyanine molecules, used on the EXAFS analysis. I, II, III, and IV are the single scattering paths (in red), while A, A', B, B', C, and C' are the multiple scattering paths (in blue the ones with 3-legs and in magenta the ones with 4)

The model for the FePc nanowires is similar to the bulk FePc, but including two FePc molecules above and below the Pc plane at a certain distance. These add a few more paths to the model: the Fe-Fe path, and a Fe-N( $v$ ) path, where the N( $v$ ) comes from the N(1) belonging to the upper or lower molecules. See Figure S3 for a scheme of these new paths. The new variables are thus the Fe-Fe distance, the horizontal shift, the Fe-Fe Debye-Waller factor, and the Fe-N( $v$ ) Debye-Waller factor, which makes a total of 14 free variables. The model for the FePcCl bulk crystal is again similar to the FePc crystal, but just adding the Fe-Cl path. This gives two more variables to the fit, the Fe-Cl distance and Debye-Waller factor, to a total of 12 variables.

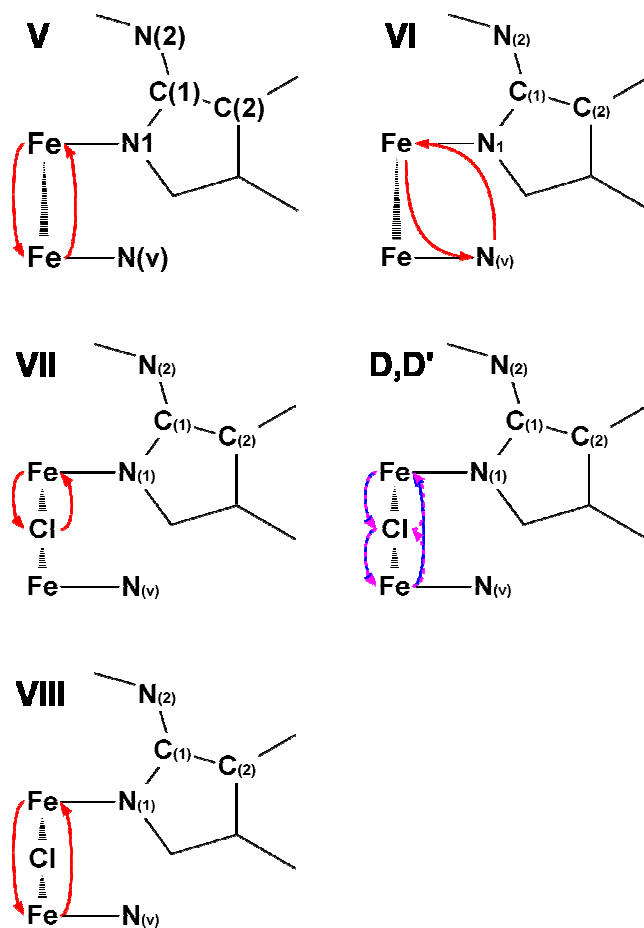


**Figure S4:** Scattering paths on the perpendicular direction of the plane of the phthalocyanine molecules, used on the EXAFS analysis. V, VI, VII and VIII are the single scattering paths (in red), while D and D' are the multiple scattering paths (in blue the one with 3-legs and in magenta the one with 4)

XAS spectra were taken from the FePc and FePcCl nanowires samples as well as from FePc and FePcCl bulk crystals for reference. Figure S4 shows the full XAS spectra from all 4 samples and Figure S5 shows the XANES region, where we can see the shoulder corresponding to the  $1s \rightarrow 3d$  transition of the Fe ions.

The software used for the analysis was the Larch 0.9 suite, which includes AUTOBK for the background subtraction and FEFF 6 for the generation of the theoretical EXAFS functions

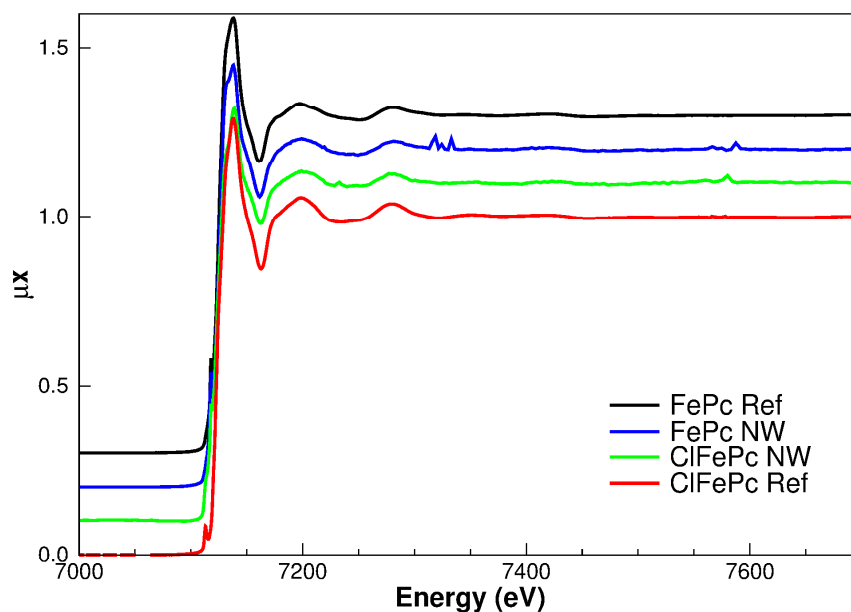


**Figure S5:** XAS spectra for the FePc and FePcCl nanowires samples (blue and green) and their corresponding FePc and FePcCl bulk crystalline reference samples (black and red).

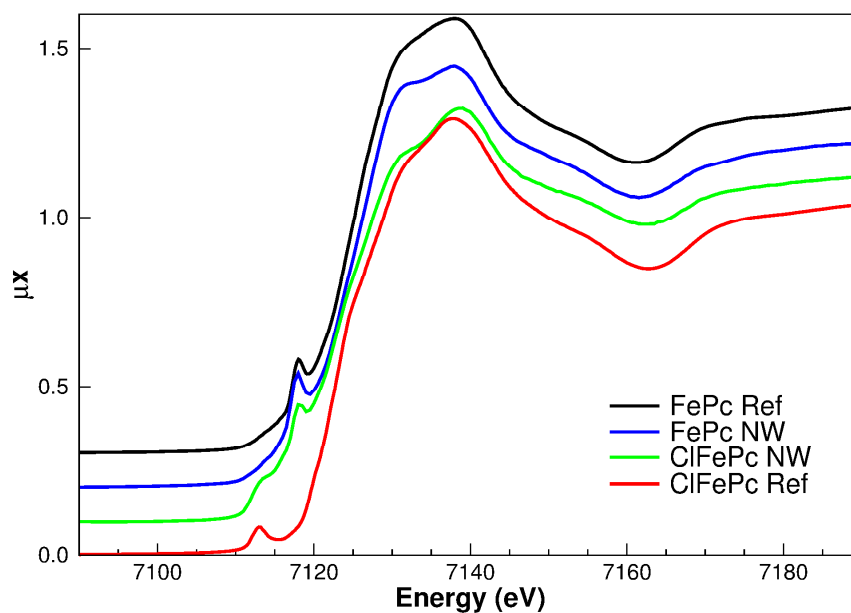


**Figure S6:** XANES region of the XAS spectra for the FePc and FePcCl nanowires samples (blue and green) and their corresponding FePc and FePcCl bulk crystalline reference samples (black and red). The characteristic pre-edge peaks can be seen between 7110 and 7120 eV, enabling the distinction between Fe(II) and Fe(III) ions.

For the FePcCl nanowire sample, we found from XANES that it consists not only of FePcCl, but also FePc. Trying to model both molecules at the same time would give an unacceptable amount of free variables, so some premises had to be made. First, we considered that both molecules are not interacting, so the nanowires are made by either FePcCl or FePc. This way, we can model each system separately, and then add up the results with a certain weight, thanks to the linearity of the EXAFS spectra. Second, we assumed that the FePc nanowires on this mixed sample are the same as the pure FePc nanowires sample, so the variables obtained at that fit (which was quite consistent and accurate) will be taken as fixed parameters for the FePc nanowire proportion of the sample. Third, the Fe-Fe distance at the FePcCl vertical stack was taken as twice the Fe-Cl distance. In this case, the scattering coming from the N(v) of the neighbor molecules is too weak to accurately determine the horizontal shift, as we did in the FePc nanowire model, so it is not taken into account. Then, only the Fe-Fe single scattering path and the co-linear multiple scattering paths Fe-Cl-Fe of three and four legs (see Figure S3) are taken in addition to the FePcCl bulk crystal model. With this premises, we just have to add two more variables to the previous model. The FePcCl:FePc ratio, and the Fe-Fe Debye-Waller factor, to a total of 14 variables.

Figure S6 shows the EXAFS signal on the k-space for all the samples, at the chosen k range of [2.5-14] Å<sup>-1</sup> along with their corresponding fits, while Figure S7 shows the Fourier transform magnitudes of these signals, again alongside with their fits.

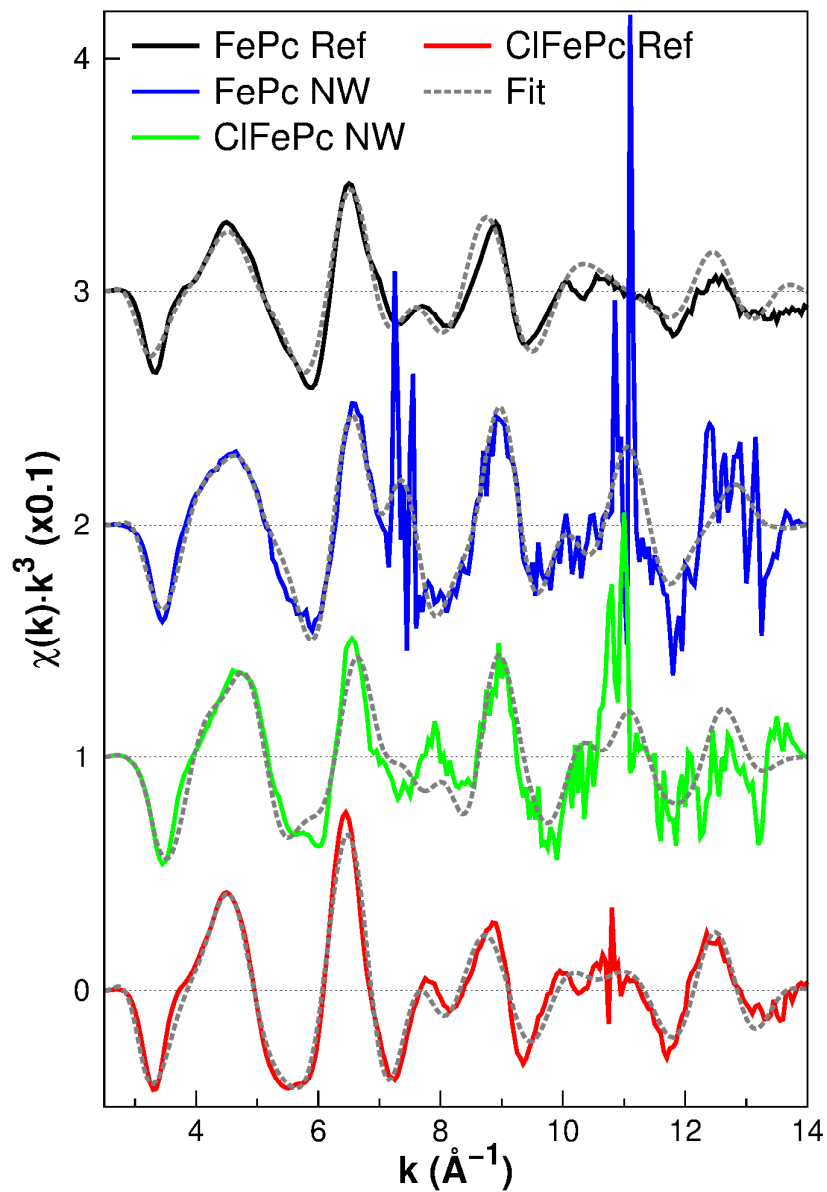


**Figure S7:** EXAFS  $\chi(k) \cdot k^3$  signal for the FePc and FePcCl nanowires samples (blue and green) and the FePc and FePcCl bulk crystalline reference samples (black and red). The respective fits are superposed in grey dashed lines.

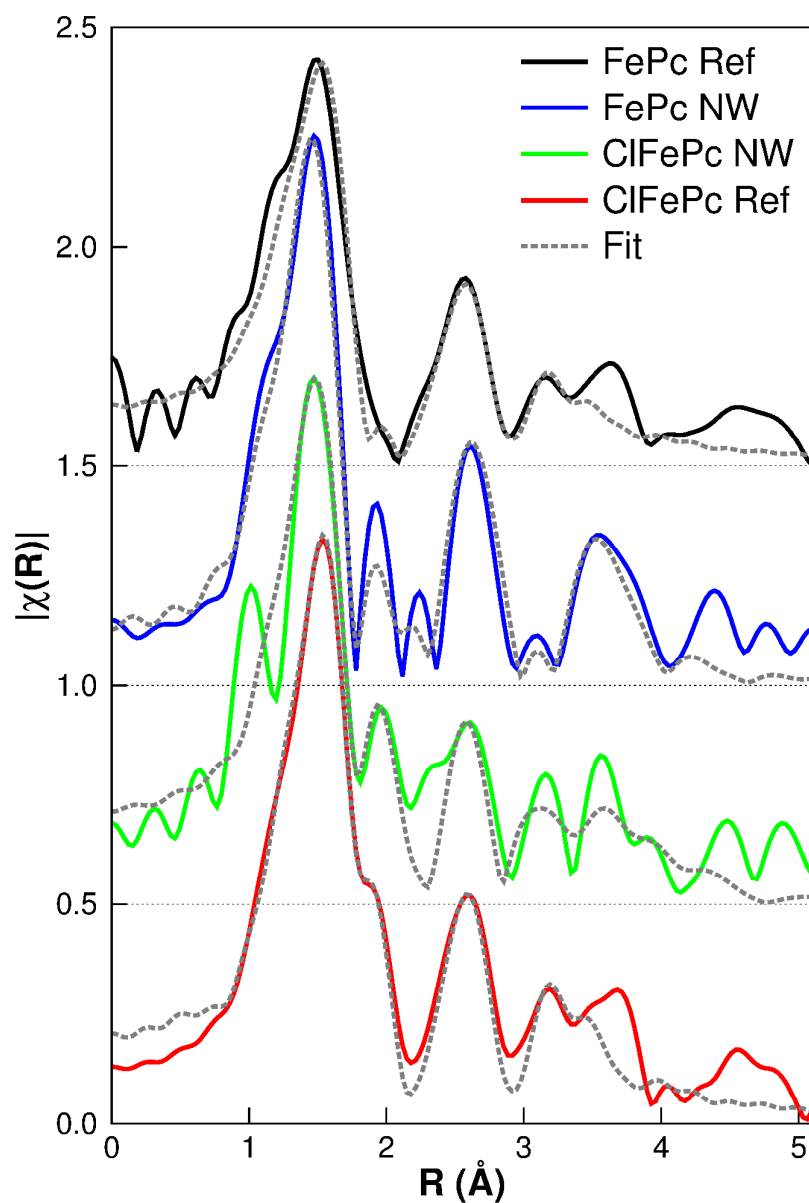


**Figure S8:** EXAFS  $|\chi(R)|$  (Fourier transform magnitude) signal for the FePc and FePcCl nanowires samples (blue and green) and the FePc and FePcCl bulk crystalline reference samples (black and red). The respective fits are superposed in grey dashed lines. The first peak on all the samples correspond to the Fe-N(1) coordination shell, while the next shoulder or close peak on the FePcCl samples at around  $2 \text{\AA}$  is the Fe-Cl shell. The next peak at  $2.5 \text{\AA}$  is the Fe-C(1) shell, and the series of peaks between  $3$  and  $4 \text{\AA}$  is a mixture of the rest of the coordination shells of the models.

The fit for the FePc bulk crystal reference is accurate up to 4 Å in the real space (Figure S7) and gives the expected results as shown in Table S2. Most of the Debye-Waller factors are relatively small, which is also expected due to the stability of this molecule, and the coordination distances only vary in the thousands of nm from the diffraction values seen in the literature.<sup>3</sup> The same happens with the FePcCl bulk crystal (Table S4). It is worth noting that both Fourier transforms look alike save from a shoulder at the right side of the first main peak, which corresponds to the Fe-Cl coordination shell, and in fact, coordination distances and Debye-Waller factors are almost the same for both models.

The fit for FePc nanowires shows a few interesting results (Table S3). First, the coordination distance of the Fe-N(2) (farther N atoms) is slightly closer (by 0.010 nm) to the Fe ion than in the bulk crystalline FePc. Second, the coordination distance of the Fe-C(2) shell (closer C atoms of the benzene rings) are quite farther (by 0.025 nm) than in the bulk FePc. These changes might come from the different interaction with the vertical stacked neighbour molecules. The two neighbour Fe atoms and their associated first N are clearly seen on the spectra, in the last peak.

The fit for FePcCl nanowires also show again differences with the bulk crystal coordination distances (Table S5). The Fe-N(2) shell is farther than the one in the bulk by 0.022 nm, while the Fe-C(2) shell is as well 0.041 nm farther than the bulk one. The stacking of these molecules on the nanowires has to be significantly different from the FePc one due to the intermediate Cl atom. Thus, this would necessarily affect the structure of the molecule, as seen in these results.

**Table S2:** Best fit structural parameters from the EXAFS analysis of the FePc bulk crystal reference sample, and the paths used for the model. Errors are in the order of 0.01Å for the coordination distances and  $1 \times 10^{-3}$  for the Debye-Waller factors.

Shell	CN	R (Å)	$\sigma^2$ ( $\times 10^{-3}$ Å <sup>2</sup> )	Paths
Fe – N(1)	4	1.96	5	I
Fe – C(1)	8	2.97	5	II, A, A'
Fe – N(2)	4	3.38	5	III
Fe – C(2)	8	4.12	15	IV, B, B', C, C'

**Table S3:** Best fit structural parameters from the EXAFS analysis of the FePc nanowires sample, and the paths used for the model. Errors are in the order of 0.01Å for the coordination distances and  $1 \times 10^{-3}$  for the Debye-Waller factors.

Shell	CN	R (Å)	$\sigma^2$ ( $\times 10^{-3}$ Å <sup>2</sup> )	Paths
Fe – N(1)	4	1.89	3	I
Fe – C(1)	8	2.96	5	II, A, A'
Fe – N(2)	4	3.27	6	III
Fe – C(2)	8	4.44	6	IV, B, B', C, C'
Fe – Fe	2	3.84	6	V
Fe – N(V)	2/4/2	4.00/4.37/4.71	6	VI

**Table S4:** Best fit structural parameters from the EXAFS analysis of the FePcCl bulk crystal reference sample, and the paths used for the model. Errors are in the order of 0.01Å for the coordination distances and  $1 \times 10^{-3}$  for the Debye-Waller factors.

Shell	CN	R (Å)	$\sigma^2$ ( $\times 10^{-3}$ Å <sup>2</sup> )	Paths
Fe – N(1)	4	1.96	5	I
Fe – C(1)	8	2.97	5	II, A, A'
Fe – N(2)	4	3.38	5	III
Fe – C(2)	8	4.09	11	IV, B, B', C, C'
Fe – Cl	2	2.25	5	VII

**Table S5:** Best fit structural parameters from the EXAFS analysis of the FePcCl nanowires sample, and the paths used for the model. Errors are in the order of 0.01Å for the coordination distances and  $1 \times 10^{-3}$  for the Debye-Waller factors.

Shell	CN	R (Å)	$\sigma^2$ ( $\times 10^{-3}$ Å <sup>2</sup> )	Paths
Fe – N(1)	4	1.93	4	I
Fe – C(1)	8	2.94	5	II, A, A'
Fe – N(2)	4	3.59	6	III
Fe – C(2)	8	4.60	6	IV, B, B', C, C'
Fe – Cl	2	2.29	13	VII
Fe – Fe	2	4.58	15	VIII, D, D'

### Chemical Characterization by X-ray Photoelectron Spectroscopy (XPS)

XPS measurements of the FePcCl nanowire sample were obtained using a XPS characterization performed in a Phoibos 100 DLD X-ray spectrometer from SPECS working in the pass energy constant mode and using the Mg K $\alpha$  as excitation source. Figure S8 gathers the most relevant peaks. Table S6 summarizes the atomic concentration for the different elements on the ClFeCl NWs sample. The Cl:Fe ratio was calculated to be 0.93, which is close to the expected 1:1.

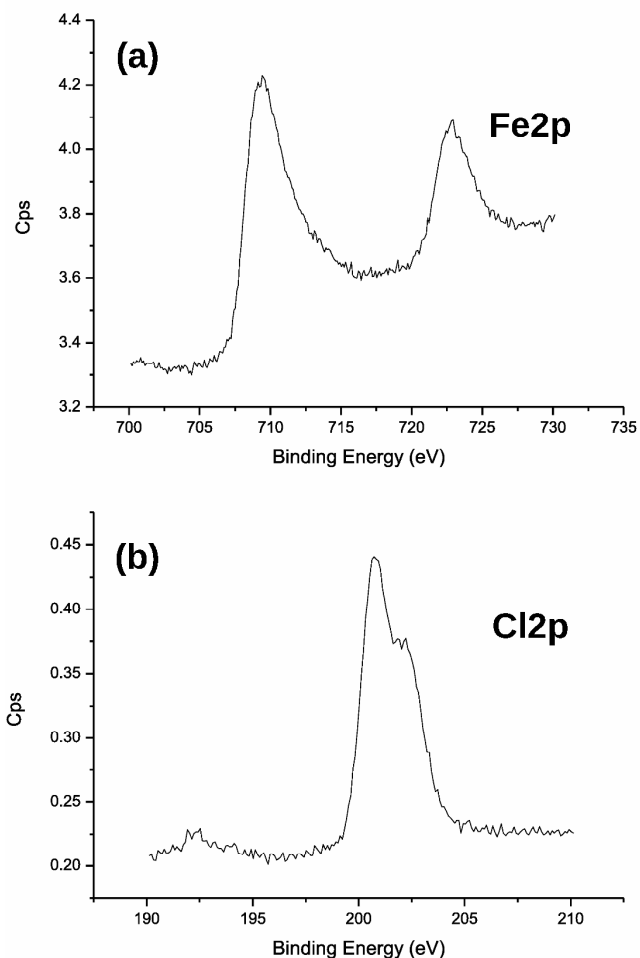


**Figure S9:** XPS spectra of the FePcI nanowire sample. (a) Detail of the Fe2p peaks. (b) Detail of the Cl2p peaks

**Table S6:** XPS quantification of the elements present on the FePcCl sample. The Cl:Fe ratio is thus 0.91, which is close to the pure FePcCl.

Element peak	Concentration (atomic %)
C1s	75.95
N1s	16.06
O1s	5.04
Cl2p	1.42
Fe2p	1.53

## References

- [1] Berger, O.; Fischer, W. J.; Adolphi, B.; Tierbach, S.; Melev, V.; Schreiber, J. Studies on phase transformations of Cu-phthalocyanine thin films. *J. Mater. Sci. in Electronics* **2000**, *11*, 331-346.
- [2] Carrera, F.; Marcos, E. S.; Merklng, P. J.; Chaboy, J.; Munoz-Paez, A. Nature of Metal Binding Sites in Cu(II) Complexes with Histidine and Related N-Coordinating Ligands, As Studied by EXAFS. *Inorganic Chem.* **2004**, *43*, 6674-6683.
- [3] Kirner, J. F.; Dow, W.; Scheidt, W. R. Molecular stereochemistry of two intermediate-spin complexes. Iron(II) phthalocyanine and manganese(II) phthalocyanine. *Inorganic Chem.* **1976**, *15*,

1685-1690.

[4] Liao, M. S.; Scheiner, S. Electronic structure and bonding in metal phthalocyanines, Metal=Fe, Co, Ni, Cu, Zn, Mg. *J. Chem. Phys.* **2001**, *114*, 9780-9791.

[5] Diaz-Moreno, S.; Munoz-Paez, A.; Marcos, E. S. X-ray Absorption Spectroscopy (XAS) Study of the Hydration Structure of Yttrium(III) Cations in Liquid and Glassy States: Eight or Nine-Fold Coordination? *J. Phys. Chem. B* **2000**, *104*, 11794-11800.

[6] Newville, M. EXAFS analysis using FEFF and FEFFIT. *J. Synchrotron Radiation* **2001**, *8*, 96-100.